MANUFACTURING TECHNOLOGY
ENGINEERING SCIENCE AND RESEARCH JOURNAL
Year 2023, Volume 23, Issue 3

ISSN 1213–2489 (print) | ISSN 2787–9402 (online)
Journal home page and articles open access: http://www.journalmt.com

Effect of Temperature and Deformation on the Stability of Retained Austenite in Closed-die Forgings from High-strength Martensitic Manganese-silicon Steels

Dagmar Bublíková (0000-0002-8684-7936), Hana Jirková (0000-0003-4311-7797), Adam Stehlík, Štěpán Jeníček (0000-0002-7492-7437)
University of West Bohemia, RTI-Regional Technological Institute, Univerzitní 22, CZ – 306 14 Pilsen, Czech Republic, e-mail: dagmar.bublikova@seznam.cz

Article abstract
In advanced steels, retained austenite is an important phase in the final microstructure, which provides a favourable combination of strength and ductility. Advanced methods capable of achieving this include the Q-P process (Quenching and Partitioning). By this means, strength of around 2000 MPa and elongation of 10-15 % can be obtained. The main factors that determine whether retained austenite remains stable in the martensitic matrix include its morphology, particle size and distribution. A closed-die forging was made from an experimental steel containing 0.42 % C, 2.45 % Mn, 2.09 % Si, 1.34 % Cr and 0.56 % Ni and Q-P processed. Based on previous data measured in a real-world process, two basic heat treatment sequences were created and tested on a thermomechanical simulator. The two sequences differed in the cooling rates. Upon heat treatment, a martensitic microstructure with a retained austenite content of 13-17 % was obtained. The ultimate strength was in the range of 2100-2200 MPa with elongations A_{5mm} 8-15 %. Austenite stability was tested by bringing the material to various temperatures (200, 300, 400, -18, -196 °C) and by cold forming at various strain rates (10^{-3}, 10^{-1}, 10 s^{-1}). The volume fraction of carbon in austenite was calculated from the lattice parameters determined by X-ray diffraction.

Keywords
Q-P process
Retained austenite
AHSS steels
X-ray diffraction
Thermomechanical simulator

DOI
10.21062/mft.2023.030

Available online
May 5, 2023

1 Introduction

Closed-die forgings from high-strength steels operate in service at various temperatures and under various loads which cause deformation. In order to achieve their required mechanical properties, such as high ultimate strength and sufficient elongation, they are treated to contain primarily a mixture of martensite and retained austenite. The stability of retained austenite significantly affects ductility. It is therefore important to know this stability at various temperatures and when subjected to various amounts of plastic deformation [1]. For the effect of austenite to be sufficiently strong, its amount in the martensitic matrix must be 10–15 %. Its stability is affected not only by its amount but also by the particle morphology and size (mechanical stability) and the levels of carbon and other alloying elements (chemical stability) [2].

Modern heat treatment of high-strength steels, which can stabilize an appropriate amount of retained austenite, include intercritical annealing and the Q&P process. Intercritical annealing is used for treating TRIP steels. It produces a mixture of bainite, ferrite and retained austenite (Fig. 1) which provide the desired mechanical properties. Intercritical annealing involves controlled cooling from the soaking temperature to holding at a bainitic transformation temperature. This route can lead to ultimate strengths up to 1500 MPa and elongation levels of about 25-40 % [3]. The other method, the Q&P (quenching and partitioning (Q&P) process, can lead to strengths of more than 2000 MPa, together with an elongation level of about 10 %. It is characterized by rapid cooling from the austenite region to a temperature between M_s and M_f. A martensitic microstructure is formed along with some amount of retained austenite. During subsequent isothermal holding, retained austenite becomes stable thanks to carbon which migrates from the super-saturated martensite to austenite. According to current knowledge, this austenite, which forms during the Q&P process, exists primarily in the form of thin films between martensite needles or plates [4]. The resulting microstructure consists of a mixture of martensite and bainite with a fraction of retained austenite (Fig. 2).

Forgings made of the steel in this study can find use in various applications and experience a variety of operating

conditions, temperatures and types of deformation. Understanding the behaviour of retained austenite under load is therefore imperative. The paper deals with the stability of retained austenite obtained during the Q&P process at different thermal and deformation loads.

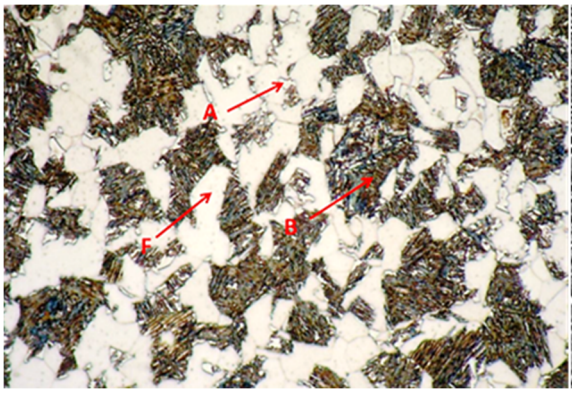

Fig. 1 *Microstructure of TRIP steel obtained by intercritical annealing, A-austenite, B-bainite, F-ferite [3]*

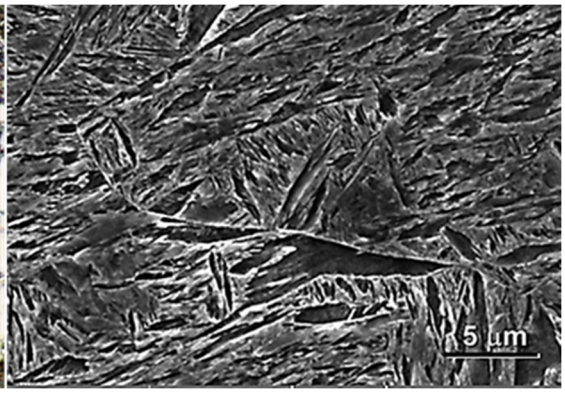

Fig. 2 *Martensitic-bainitic microstructure with amounts of retained austenite after Q&P processing*

2 Materials and Methods

Selection of material

For this experiment, a martensitic steel was created with 0.4 % carbon and a special alloying intended to depress the M_s and M_f temperatures (Tab. 1). The main alloying element in this steel is manganese. Manganese was added in order to lower the M_s and M_f temperatures and to shift the ferrite and pearlite nose towards lower cooling rates in transformation diagrams. Manganese further improves hardenability of solid solution. Another alloying element was silicon, which prevents undesirable carbides from forming, and therefore leads to supersaturation of martensite with carbon. It promotes carbon diffusion in martensite and thus stabilizes retained austenite [5, 6]. Chromium was added to improve hardenability and strength. The prerequisite for improved hardenability, however, is that the carbides dissolve during austenitizing. Undissolved carbides act as nuclei and reduce hardenability. Molybdenum depresses the M_s a M_f temperatures and make martensite more stable [6]. Nickel, even in small amounts, serves the purpose of stabilising retained austenite and providing better hardenability. Niobium belongs to the most widely-used microalloying elements [7]. Even a minute amount substantially alters mechanical properties of steel. Niobium has a strong affinity for carbon and nitrogen. They combine to form carbonitrides which dictate mechanical properties of the material. Niobium dictates the type of austenite, most notably in TRIP steels. For niobium-free steels it is mainly a granular type, steels alloyed with niobium contain so-called interlath form of austenite [8]. Transformation temperatures M_s and M_f were calculated from chemical composition using JMatPro software as 209 °C and 78 °C, respectively.

Tab. 1 *Chemical compositions of the experimental AHSS [wt. %]*

C	Mn	Si	P	S	Cu	Cr	Ni	Al	Mo	Nb	M_s [°C]	M_f [°C]
0.419	2.45	2.09	0.005	0.002	0.06	1.34	0.56	0.005	0.04	0.03	209	78

Stability of retained austenite at various temperatures and upon cold deformation

Since high-strength steel components are used at various temperatures, it is necessary to know the retained austenite stability at temperatures other than room temperature. Using real-world data measured by a thermocouple during the Q&P process on closed-die forgings, two basic sequences for a thermomechanical simulator were developed. They had different rates of cooling from the soaking temperature to the quenching temperature (Tab. 2). They matched the rates of cooling the forging's surface and interior in hot water (Fig. 3). The specimens treated with these sequences were used for testing the stability of retained austenite at various temperatures.

They were heated in a furnace without protective atmosphere to 200, 300 and 400 °C, held for 60 minutes and cooled in still air. Furthermore, cooling to -18 °C and cooling in liquid nitrogen to -196 °C were applied, with a hold of 60 minutes (Tab. 3). The measured amounts of retained austenite were compared between these specimens and the initial condition (Tab. 2).

Mechanical properties of steels which contain retained austenite are also affected by the speed of transformation of retained austenite to strain-induced martensite when the steel is subjected to plastic deformation. The strain rate involved is important as well. Specimens treated in the thermomechanical simulator were compressed with a strain magnitude of $\varphi = 0.13$ at room temperature at various strain rates (10^{-3}, 10^{-1}, 1 s^{-1}), (Tab. 4). After this deformation, the retained austenite volume fraction was measured by X-ray diffraction once again and compared with the value prior to deformation (Table 2).

Based on austenite lattice parameters determined by X-ray diffraction, the volume fraction of carbon in austenite was calculated for the initial condition, for various thermal exposures and during cold deformation using equation (1). This equation is a combination of the Ruhl and Cohen method for manganese, silicon and carbon and the Dyson and Holmes method for aluminium [9], Tab. 2, 3, 4.4

Tab. 2 *Heat treatment routes and results of mechanical testing*

Sequence number	T_A[°C]/t_A [s]	Cooling rate [°C/s]	QT [°C]	PT [°C/s] /t_{PT} [s]	HV10 [-]	R_m [MPa]	A_{5mm} [%]	RA [%]	α [nm]	C [wt%]
1	880/2400	64	100	200/3600	637	2114	15	17	0,35880	0,49
2		5.7	244	200/3600	669	2250	8	13	0,35901	0,56

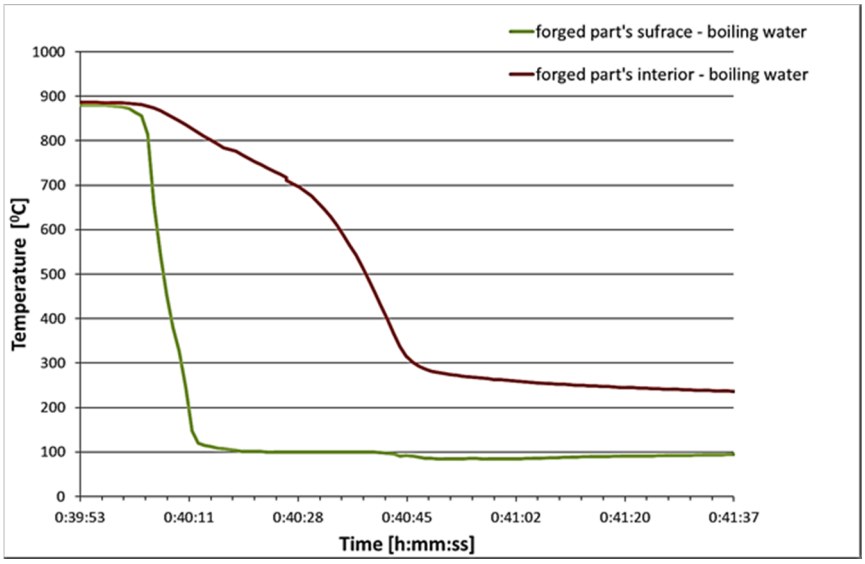

Fig. 3 *Cooling curves of the forged part's surface and interior in boiling water*

Tab. 3 *Results of X-ray diffraction at various thermal exposure and hardness data*

Regime number	Exposure temperature [°C]	Time at temperature [s]	HV10 [-]	RA [%]	α [nm]	C [wt%]
1	200	3600	596	13	0.35878	0.49
2			630	10	0.36029	0.95
1	300		573	17	0.36007	0.88
2			605	10	0.36097	1.15
1	400		562	15	0.36014	0.9
2			586	11	0.36021	0.92
1	-18		605	15	0.35882	0.5
2			649	13	0.35995	0.84
1	-196		609	13	0.35877	0.52
2			663	8	0.35978	0.79

Tab. 4 *Retained austenite fraction depending on the amount of strain and results of mechanical tests*

Sequence number	Strain rate [s^{-1}]	HV10 [-]	Red. of area [%]	α [nm]	C [wt%]
1	10^{-3}	617	13	0.35971	0.77
2		673	8	0.36025	0.93
1	10^{-1}	625	12	0.35915	0.61
2		667	9	0.36214	1.51
1	1	655	11	0.35941	1.14
2		677	7	0.36093	1.14

$$\boldsymbol{\alpha = 3,572 + 0,0012(wt\ Mn) - 0,00157(wt\ Si) + 0,0056(wt\ Al) + 0,033(wt\ C)}\text{Å}\ \mathbf{(1)}[9],$$

α – lattice parameter [Å]

wt – fractions of individual elements in weight percent [wt %]

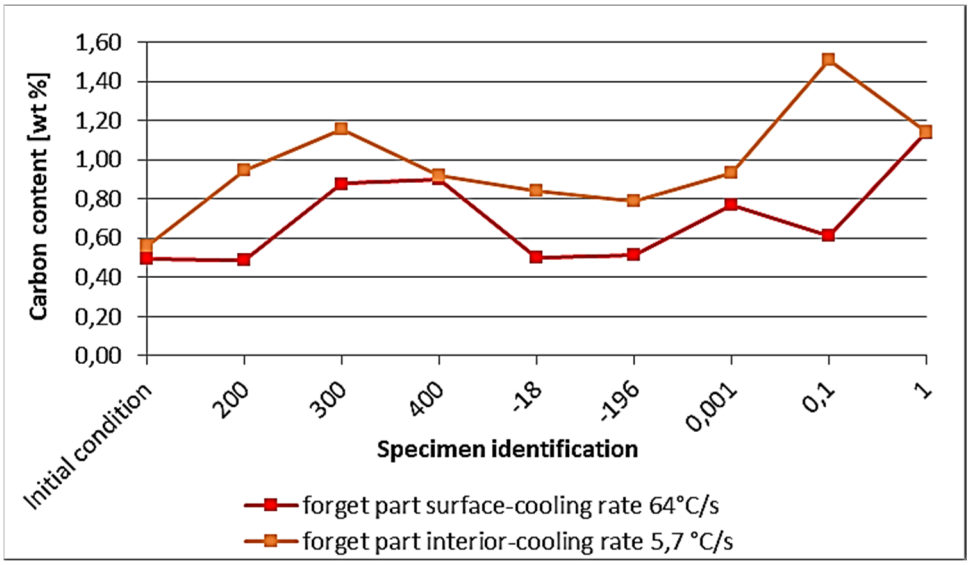

Fig. 4 *Share of retained austenite at various temperatures and upon cold deformation*

Discussion of results

Two heat treatment sequences with different cooling routes led to a martensitic-bainitic microstructure with 17 % and 13 % retained austenite. The sequence with the cooling rate of 64 °C/s led to an ultimate strength of 2114 MPa and an elongation of 15 % (Tab. 2). Hardness was 637 HV10. For the sequence with the slower cooling rate of 5.7 °C/s, ultimate strength was 2255 MPa and elongation reached 8 %. Hardness was 669 HV10. From the data collected through thermocouples, it was found that the forgings' interior did not reach M_s during cooling and quenching finished at 244 °C. Therefore, martensite only formed during cooling down from the partitioning temperature and was not tempered. Fresh martensite was identified in the microstructure, which corresponds to higher levels of strength and hardness.

The specimens from these two basic sequences were used for testing the stability of retained austenite at various temperatures. Upon the exposure of the specimens to 200 °C, no substantial microstructural changes were detected. In both cases, the resulting microstructure was again a mixture of martensite and bainite with a lower fraction of retained austenite, 13 % and 10 % (Fig. 4. a, b). The microstructure only became slightly tempered, which led to lower hardness levels: 596 and 630 HV10 (Tab. 3), when compared to the initial condition (637 and 669 HV10 (Tab. 2). Upon the exposure to 400 °C, strong effects of tempering were observed and the resulting microstructure consisted of a mixture of ferrite and cementite with a sorbitic morphology (Fig 5. a, b). This was reflected in lower hardness levels: 561 and 586 HV10 (Tab. 3). Although hardness dropped after the thermomechanical simulation, austenite remained very stable and did not decompose to martensite when cooled to room temperature. After thermal exposure at 400 °C, retained austenite fraction was 15 % in the specimens treated earlier by cooling at 64 °C/s and 11 % in specimens cooled earlier at 5.7 °C/s. This may be due to carbon and other alloying elements partitioning from super-saturated martensite to austenite, which contributes to its stability.

Where the material was exposed to below-zero temperatures, no substantial changes in the microstructure were

found (Fig. 6. a, b.). It appears that cooling the specimens to -18 °C has not brought them below the M_s temperature of retained austenite. The amount of retained austenite was approximately 5 % less in both conditions under test. Quenching in liquid nitrogen at -196 °C led to a slightly lower amount of retained austenite (8 %). In route 2, which was equivalent to the cooling process in the interior of the forged part, supercooling caused a portion of austenite to transform to martensite.

For both sequences, the stability of the retained austenite was tested by upsetting the specimens at various strain rates. The microstructure was a mixture of martensite, bainite and retained austenite (Fig. 7. a, b). Work hardening was induced by deformation, which led to an increase in hardness (Tab. 4). Hardness rises significantly with increasing strain rate (up to 1 s^{-1}), most notably in the specimens from sequence 1 which involved a relatively higher cooling rate. At the highest strain rate, most retained austenite transformed to martensite. Despite the high strain rate, some amount of retained austenite remained in all specimens (11 % and 7 %, Tab. 4).

Using the lattice parameters, the volume fraction of carbon in austenite for various thermal exposures and after cold deformation was calculated (Tab. 3, Tab. 4). With increasing heating temperature, carbon migrated from super-saturated martensite to retained austenite. As a result, the lattice parameter of retained austenite increased, which means that the carbon content in austenite increased (Tab. 3, Fig 4). The fact that austenite remained stable even after various thermal exposures indicates that it was sufficiently saturated with carbon, and therefore it did not transform into martensite during subsequent cooling. The specimens treated with the sequence with a lower cooling rate did not reach M_s temperature during quenching. Hence, it was only the thermal exposure which caused tempering of martensite and significant saturation of austenite with carbon. For this reason, the increase in the carbon content in austenite with the temperature of thermal exposure was much steeper than in specimens which had been cooled more slowly. The maximum was reached at thermal exposure at 300 °C, when the carbon content in austenite was up to 1.15 % (Tab. 3, Fig. 4). At a thermal exposure temperature of 400 °C, the carbon content decreased, which may indicate partitioning of alloying elements between austenite and martensite.

During cold compressive deformation, a certain amount of austenite was transformed to martensite, resulting a lower amount of retained austenite. Austenite did not completely transform during deformation. Islands of the so-called M-A constituent, where austenite partially transformed to martensite, formed in the microstructure. Due to the deformation, lattice deformed as well (Tab. 4). This led to a gradual increase in the lattice parameter of austenite.

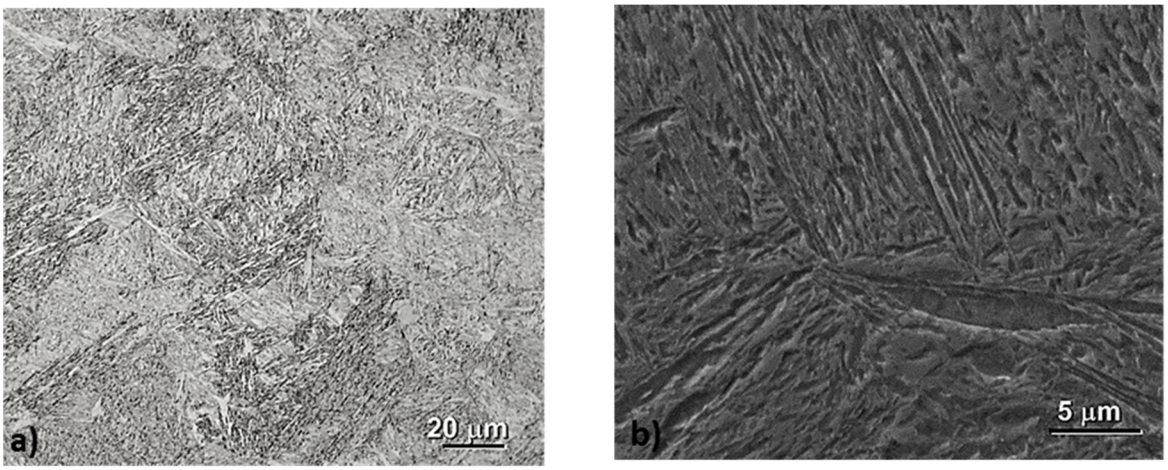

Fig. 5 *Sequence 1, cooling rate 64 °C/s, thermal exposure 200 °C, martensitic microstructure with some amount of bainite and retained austenite, a) optical micrograph (OM), b) SEM close-up view*

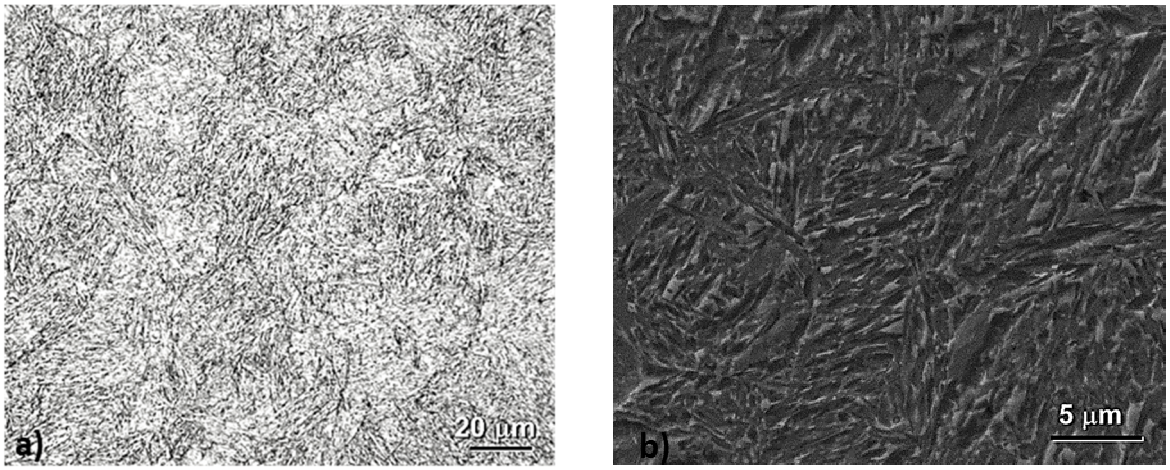

Fig. 6 *Sequence 2, cooling rate 5.7 °C/s, heating temperature 400 °C, sorbite close-up view a) OM, b) SEM detail*

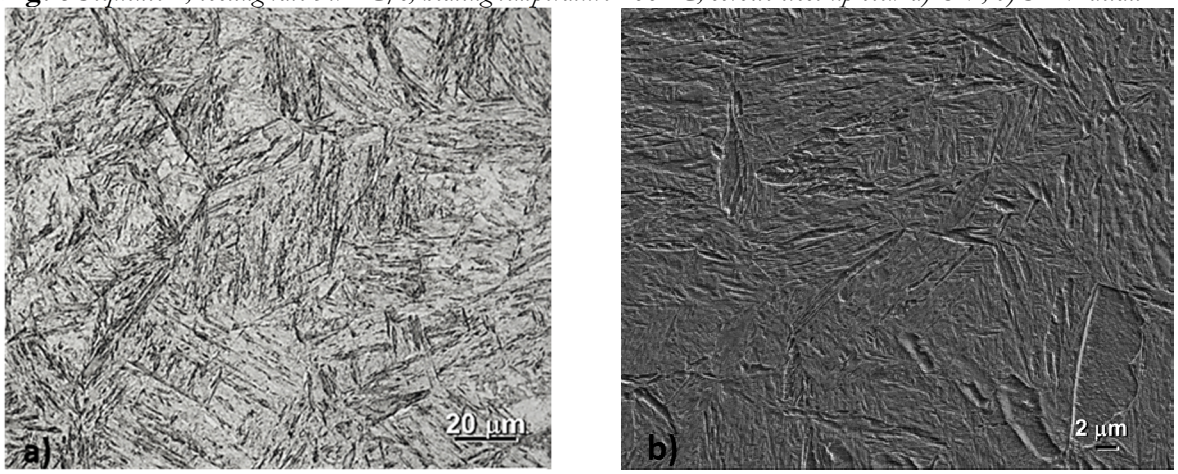

Fig. 7 *Sequence 2, cooling rate 5.7 °C/s, -196 °C, martensitic microstructure with some amount of bainite and austenite, a) OM, b) SEM close-up view*

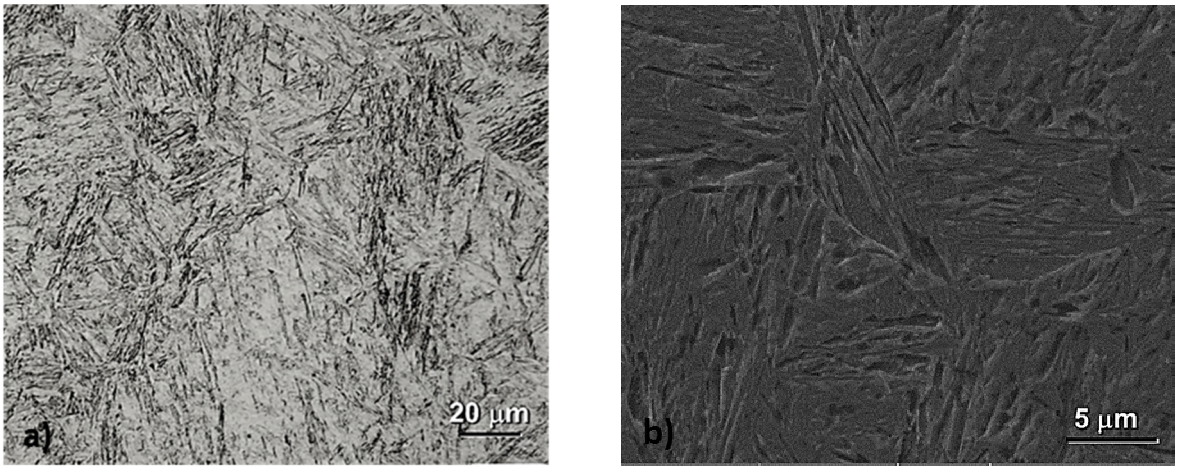

Fig. 8 *Sequence 2, cooling rate 5.7 °C/s, strain rate 1 s^{-1}, martensitic microstructure with some amount of bainite and retained austenite, a) OM, b) SEM close-up view*

3 Conclusion

Since products made as closed-die forgings operate at various temperatures and are subject to various kinds of deformation, the stability of retained austenite at multiple temperatures and during cold deformation was tested. Thermal stability of austenite was tested by exposure at -196 to 400 °C for 1 hour. Relatively large amounts of retained austenite remained in specimens from both sequences after all thermal exposures. Changes in the mixed martensitic microstructure first occurred at 300 °C, when tempering transformed martensite to a mixture of ferrite and cementite (sorbite), and the hardness dropped to 560 HV10.

Where compression was applied, the strain rate affected the transformation of retained austenite to martensite.

At the highest strain rate of 10 s^{-1}, the amount of retained austenite for both sequences decreased to 11 % and 7 % due to transformation. Higher amount of martensite and strain hardening led to an increase in hardness to 670 HV10.

The stability of retained austenite after thermal exposures was confirmed by calculating the volume fraction of carbon in austenite using calculated lattice parameters. As the exposure temperature increased, diffusion raised the carbon content in austenite. Upon cold compressive deformation, not only partial transformation of austenite to martensite but also distortion of the lattice occurred. This resulted in an increase of lattice parameter of austenite.

Acknowledgements

This paper includes results achieved within the project SGS-2021-025. Electron beam application for welding advanced high strength steels. The project is subsidised from specific resources of the state budget for research and development.

References

[1] BUBLÍKOVÁ, D., MAŠEK, B., VOREL, I., JENÍČEK Š. (2017). Stability of retained austenite in hight-strenght martensitic steel with low M_s Temperature, *Manufacturing Technology*, Vol. 17, No 4, pp. 428–433.

[2] MAŠEK, B., JIRKOVÁ, H., HAUSEROVÁ, D., KUČEROVÁ, L., KLAUBEROVÁ D. (2010). The Effect of Mn and Si on the Properties of Advanced High Strength Steels Processed by Quenching and Partitioning, *Materials Science Forum*, Vol. 654-656, pp. 94-97.

[3] QIAN, Z., LIHE Q., JUN T., JIANGYING M., FUCHENG Z. (2014). Inconsistent effects of mechanical stability of retained austenite on ductility and toughness of transformation-induced plasticity steels, *Materials Science & Engineering A*, Vol. 578, pp. 370–376.

[4] JIRKOVÁ, H., et al. (2014). Influence of metastable retained austenite on macro and micromechanical properties of steel processed by the Q-P process, *Journal of Alloys and Compounds*, available online, Journal of Alloys and Compounds, Vol. 615, pp. 163–168.

[5] PEKOVIĆ, M., VOREL, I., KÁŇA, J., OPATOVÁ, K., (2017). Evolution of microstructure and mechanical properties in steels during isotermal holding in the region of bainitic transformation temperature in dependence on silicon content, *Manufacturing Technology*, Vol. 17, No. 2, pp. 549-555.

[6] BAIK, S. CH., KIM, S., JIN, S., KWON, O. (2001). Effect of alloying elements on mechanical propeties and phase transformation of cold rolled TRIP steel steels, ISIJ International, Vol. 41, No. 3, pp. 290-297.

[7] SEJČ, P., JAŠKO, P., BAXA, P., BELANOVÁ, J. (2017). Stability of Ni/TiB_2 coating on CuCrZr Electrodes for resistence spot welding galvanized steeel sheet, *Manufacturing Technology*, Vol. 17, No 4, pp. 570-576.

[8] PARK, S. H., CHOO, W. Y., KIM, N. J., KO, J. H. (1996). Effects of hot rolling conditions on the microstructure and tensile properties of Nb-bearing TRIP steels, International Symposium on Hot Workability and Light Alloys Composites, TMS of CIM, Motrioll Quebek, Canada, pp. 493.

[9] TAKAHASHI, M., YOSHIDA, H., HIWATASHI, S. (2002). International Conference on trip aided hight strength ferrous alloys, proceedings on CD, Ghent, Belgium, pp. 103-111.